

REPORTS

SIGNAL PROCESSING

Subnoise detection of a fast random event

V. Ataie, D. Esman, B. P.-P. Kuo, N. Alic, S. Radic*

Observation of random, nonrepetitive phenomena is of critical importance in astronomy, spectroscopy, biology, and remote sensing. Heralded by weak signals, hidden in noise, they pose basic detection challenges. In contrast to repetitive waveforms, a single-instance signal cannot be separated from noise through averaging. Here, we show that a fast, randomly occurring event can be detected and extracted from a noisy background without conventional averaging. An isolated 80-picosecond pulse was received with confidence level exceeding 99%, even when accompanied by noise. Our detector relies on instantaneous spectral cloning and a single-step, coherent field processor. The ability to extract fast, subnoise events is expected to increase detection sensitivity in multiple disciplines. Additionally, the new spectral-cloning receiver can potentially intercept communication signals that are presently considered secure.

The spontaneous decay of a molecule (1), a fast radio-astronomy burst (2), or the arrival of a secure communication packet (3) are examples of nonrepetitive events that pose similar challenges for observers. In addition to requiring a fast and sensitive detector, a randomly occurring signal must be extracted from the background noise in either the optical or electrical domain. If the event is repetitive, this noise can be substantially eliminated by classical averaging (4). When noise is temporally uncorrelated, the summation of a sufficiently large number of signal instances can lead to an arbitrary signal-to-noise ratio (SNR) improvement (4). Simple to implement, averaging plays a critical role in the capture of fast, weak, or noisy signals. A powerful generalization of the averaging concept was developed for cyclostationary signals accompanied by spectrally uncorrelated noise (5). In contrast to temporal averaging, cyclostationary and cumulant analysis recognizes that noise spectral components can be rejected if the signal is cyclically modulated. Intuitively, a similar treatment could be extended to a single-instance signal if it can be temporally replicated. In earlier work (6), a recirculating loop was used to create multiple, serialized signal outputs that can be independently detected and subsequently averaged. Such replication requires an amplifier to overcome coupling losses, thus injecting excess (amplification) noise. Unfortunately, all known temporal replication mechanisms (6, 7) are inherently lossy and are subject to this basic limitation.

However, a single event can be replicated to frequency nondegenerate copies (spectral clones) in a nearly noiseless manner (8). We show that an isolated pulse can be extracted from noise by single-step processing of its spectral clones. To

demonstrate single-event detection, an 80-ps-long pulse was cloned and processed in order to increase the received SNR by 14.1 dB. To separate signal from noise, the experiment varied the number of spectral copies from 6 to 36, proving that background rejection can be progressively increased even when the random event is immersed in a high level of background noise.

When a repetitive signal $s(t)$ is accompanied by noise $n(t)$, its estimate can be reached by coherent summation (4): $\sum_{k=1}^N \frac{1}{N\Delta T} \int_{t_k-\Delta T/2}^{t_k+\Delta T/2} [s(t) + n(t)] dt$, where t_k and ΔT indicate the signal instance and observation (detection) interval, respectively. For a sufficiently large occurrence count ($N \gg 1$), when noise is a zero-mean uncorrelated process (4), this estimate can be arbitrarily accurate because $\sum_{k=1}^N \frac{1}{N\Delta T} \int_{t_k-\Delta T/2}^{t_k+\Delta T/2} n(t) dt \rightarrow 0$. In the case of a single event ($N = 1$), noise cannot be repeatedly measured but can still be discriminated from the signal in the spectral domain. Indeed, whereas two distinct signal spectral components have a deterministic relation, the same is not true for noise components. This important difference was recognized (5) and used to discriminate δ -correlated noise from the signal. In the simplest cyclostationary receiver implementation, the product of two spectral components is integrated over many signal cycles in order to acquire the correlation between any pair of spectral components. The correlation collapses when only noise is received, thus allowing for signal feature extraction (5).

Cyclostationary detection fails to reject the noise accompanying an isolated (single-cycle) event because no correlation can be drawn at any time instance beyond the event duration. However, by replicating such a signal in a substantially noiseless manner, one can still exploit the fact that the signal possesses spectral correlation, whereas the received noise does not (Fig. 1). To describe noise discrimination in

this case, let us assume that a set of lossless narrow filters with bandwidth δf can be constructed over the full span of a Δf -wide signal (Fig. 1). The spectral decomposition (9) of the received field $r(t) = s(t) + n(t)$ can be described by the short-time Fourier transform (STFT)

$$R(t, k\delta f) = \int_{-1/2\delta f}^{+1/2\delta f} w(t-\tau)r(\tau)e^{j2\pi k\delta f\tau} d\tau, \text{ where}$$

$w(t) = \sin(\pi\delta f t)/\pi t$ is the δf -wide band-pass window function. STFT is a slowly varying complex function that, when sampled within the detection interval $[t \pm 1/(2\delta f)]$ (9), represents the received spectral component centered at f_k as the phasor sum $\mathbf{R}_k = \mathbf{S}_k + \mathbf{n}_k$. In the absence of noise, its magnitude is a measure of the signal spectral density $\hat{S}(f_k)$; in the absence of the signal, the magnitude and phase of this phasor is defined by the statistics of the interfering noise field.

The STFT cannot be realized by mere filtering centered at f_k because it will result in the carrier-specific phase rotation $2\pi f_k t$. To address this, the differential phasor rotation must be stopped by frequency shifting each output to the baseband (9). Consequently, phasor summation across the entire bandpass set leads to a noise-sensitive outcome. For a noiseless, transform-limited signal pulse, this summation results in collinear vector addition. In contrast, when only noise is present this summation resembles a random walk in the complex plane, (Fig. 1, inset Σ). Consequently, the effective SNR increase provided by a spectrally cloning detector should scale with the replica count N as $\sim (N/\sqrt{N})^2(10)$.

Although the single-event detector is conceptually simple, its realization faces a set of basic challenges. In the first of these challenges, the spectral decomposition process must be distortionless and lossless. This requirement is easily satisfied for slow, microsecond-scale events that can be quantized with high precision (11, 12). In this case, the digitized field can be used to calculate the sampled STFT and emulate the coherent subband summation (Fig. 1). However, when the event is fast (subnanosecond), signal quantization imposes a fundamental resolution limit (11, 12), eliminating such a computational approach. Its alternative, physical channelization (13), is neither distortionless nor lossless.

Recognizing these limits, we mapped the received signal onto widely separated frequency carriers (ΔF) and performed spectral decomposition by means of a strictly periodic bandpass process (Fig. 1). In the optical domain, the received spectrum can be parametrically cloned (8) and subsequently decomposed by a single physical filter (14). This strategy cannot be applied in spectral ranges where efficient, low-noise parametric mixers (15, 16) do not exist. Among those ranges, the microwave range (0.3 to 100 GHz) is arguably the most important because it hosts commercial (17), scientific (17), and defense (17, 18) signals. To construct a single-event detector operating in this band, we mapped the received field onto a highly coherent frequency comb (Fig. 2).

In the first experiment, a single-instance signal was represented by a 12-GHz-wide pulse and was

Department of Electrical and Computer Engineering, University of California, San Diego, La Jolla, CA 92093, USA.
*Corresponding author. E-mail: sradic@ucsd.edu

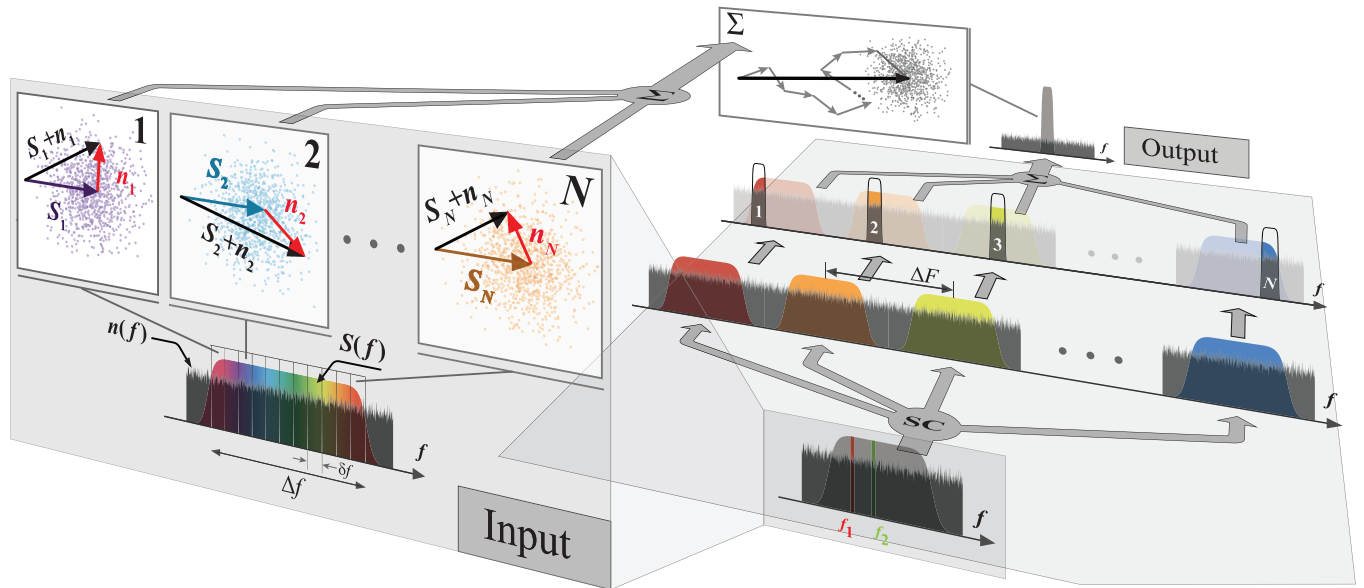


Fig. 1. Single-event noise discrimination. A set of lossless bandpass filters (δf) spectrally decomposes the signal and noise fields into a set of \mathbf{S}_k and \mathbf{n}_k phasors. In the reference frame of the signal carrier, these phasors are not synchronous and rotate at different rates $\omega = 2\pi f_k$ ($k = 1, N$); Spectral cloning (SC) maps the received field onto a widely spaced grid (ΔF) and enables lossless spectral decomposition by means of a single periodic process (filter). To coherently sum signal (noise) phasors, differential phasor rotation must be arrested by means of a frequency-invariant baseband process.

cloned to six spectral replicas. The pulse was centered at 6.5 GHz and combined with broadband noise generated by a photodiode that receives amplified spontaneous emission from an erbium-doped fiber amplifier. The signal and noise were combined and used to modulate a tunable optical frequency comb (TOC_1), replicating the noise-loaded signal onto its frequency modes. Each mode had an optical SNR in excess of 40 dB, measured within a 12.5-GHz bandwidth and at 1550 nm. TOC_1 had a continuously variable frequency pitch (19) that was set to $\Delta F = 50$ GHz. The second (Vernier) optical comb (TOC_2) was used as a local-oscillator (LO) array, with frequency pitch differing by $\delta f = 2$ GHz from the signal comb. Both optical combs were seeded by a single master oscillator with a spectral linewidth of 3 kHz, guaranteeing a high degree of mutual coherence (20) during the longest signal capture time (~ 256 μs). The ability to continuously tune the frequency pitch of both optical combs is critical because it defines the offset between a specific spectral replica and the distinct LO mode. When combined in a detector with bandwidth δf_D , the beating between the k^{th} replica and the LO mode selects a δf_D -wide spectral segment that is centered $f_k = k \times \delta f$ away from the replica carrier. If the detector bandwidth and the comb frequency offset are matched ($\delta f_D = \delta f$), the comb-assisted cloning becomes equivalent to the spectral decomposition (Fig. 1). Two wavelength-demultiplexing elements (WDMs) were used to route the spectrally overlapping copy and LO mode to a coherent detector (D). A matched detector bandwidth, defined by the ratio of the pulse bandwidth ($\Delta f = 12$ GHz) and the spectral replica count $N = 6$, defines the frequency offset between the signal (TOC_1) and Vernier combs (TOC_2), $\delta f = \Delta f/N = 2$ GHz. Last, the output of each detector D is sampled and used

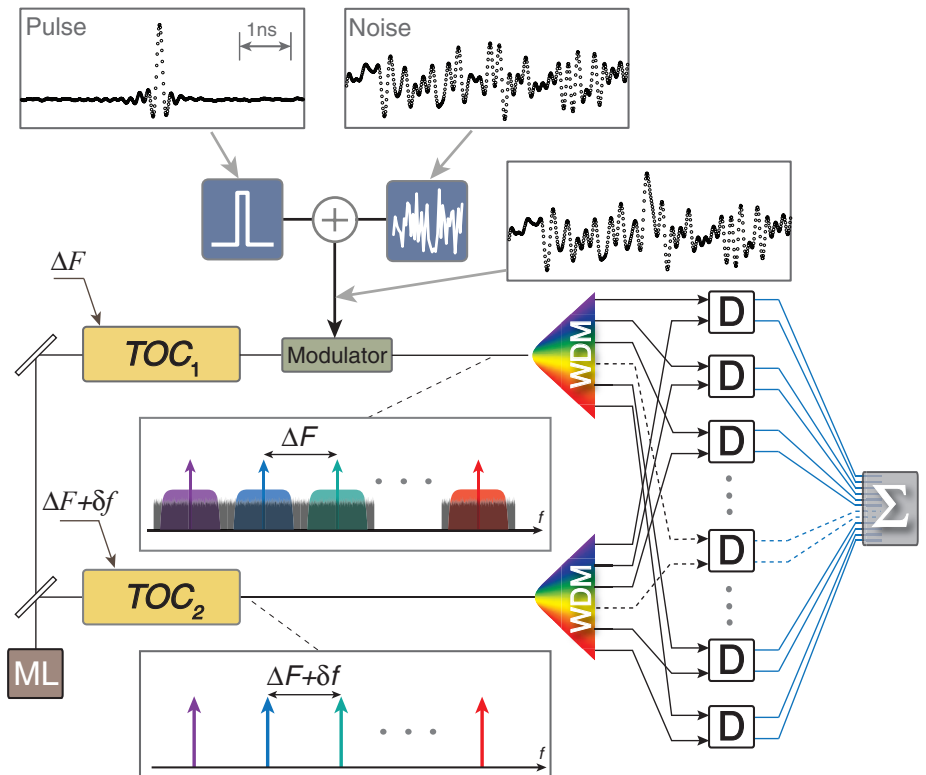


Fig. 2. Spectral cloning receiver. Two frequency-tunable optical combs (TOC_1 and TOC_2) are derived from a single master laser (ML). A single pulse is combined with noise and used to modulate TOC_1 with frequency pitch ΔF . The Vernier comb TOC_2 , with frequency pitch $\Delta F + \delta f$, serves as local oscillator array and is combined with the received signal at the substrate detector array (D).

to perform coherent summation in order to discriminate the pulse from the noise, as detailed in (27).

The first measurement generated six spectral copies of an 80-ps pulse accompanied by various

levels of interfering noise (Fig. 3A). The input SNR (SNR_{IN}) was defined as the ratio of the signal and noise powers, measured within the observation interval $N/\Delta f = 500$ ps. We performed

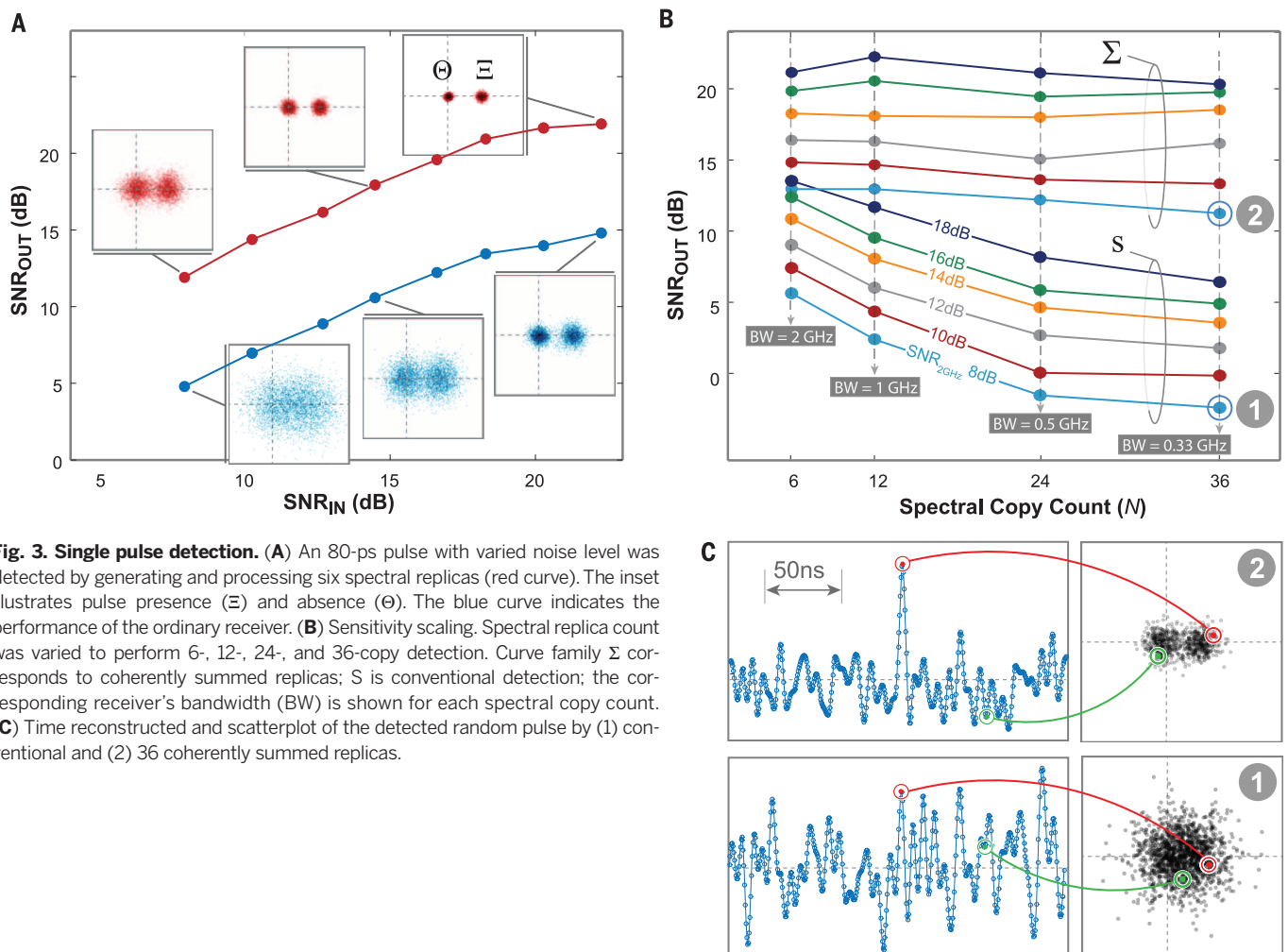


Fig. 3. Single pulse detection. (A) An 80-ps pulse with varied noise level was detected by generating and processing six spectral replicas (red curve). The inset illustrates pulse presence (Ξ) and absence (Θ). The blue curve indicates the performance of the ordinary receiver. (B) Sensitivity scaling. Spectral replica count was varied to perform 6-, 12-, 24-, and 36-copy detection. Curve family Σ corresponds to coherently summed replicas; S is conventional detection; the corresponding receiver's bandwidth (BW) is shown for each spectral copy count. (C) Time reconstructed and scatterplot of the detected random pulse by (1) conventional and (2) 36 coherently summed replicas.

4720 detections to quantify the ability to distinguish signal from noise. Measurements (Fig. 3A) are shown with each point in the scatter plot corresponding to a single detection outcome. Intuitively, the detection of a low-noise pulse corresponds to highly distinguishable ensemble scatters. As an example, the measurement ensemble Ξ (Fig. 3A) corresponds to the detection of a signal with $\text{SNR}_{\text{IN}} = 22.3$ dB, whereas in Θ , the signal was absent. The less overlap between these scatters reflects a higher confidence level (22) with which one can differentiate between pulse presence and absence, as detailed in (2I). To quantify the spectral-cloning receiver performance, we define the output SNR (SNR_{OUT}) as the ratio between the square of the scatter mean separation and its variance. As an illustration, a pulse with $\text{SNR}_{\text{IN}} = 7.9$ dB is detected with $\text{SNR}_{\text{OUT}} = 11.9$ dB, indicating a 4-dB increase in the level of detection confidence. To compare the performance of the spectral cloning and conventional detector, we did not perform coherent decomposition and summation in a subsequent set of measurements. Instead, the output of each detector was recorded and its average was plotted (Fig. 3A). The increase in SNR_{OUT} between the two cases varies from 7.1 dB ($\text{SNR}_{\text{IN}} = 22.3$ dB) to 7.5 dB ($\text{SNR}_{\text{IN}} = 18.3$ dB), which is in agreement with the

value predicted previously for six ($N = 6$) spectral replicas $\sim (N/\sqrt{N})^2 \sim 7.8$ dB.

Last, to test the main hypothesis, which predicts that the sensitivity increases with spectral clone count, we constructed receivers with 12, 24, and 36 replicas. To circumvent the physical scaling of the substrate detector array, interfering noise was synthesized by using a 64-GS/s digital-to-analog-converter (DAC) and combined with a 12-GHz-wide pulse, as described in (2I). Clone-scaling measurements (Fig. 3B) indicate that an average sensitivity gain of 10.4, 13.1, and 14.1 dB was achieved when 12, 24, and 36 copies were generated, respectively. These measurements agree remarkably well with the predicted sensitivity gains $(N/\sqrt{N})^2 \sim 10.8, 13.8,$ and 15.6 dB, when $N = 12, 24,$ and $36,$ respectively.

These results prove the importance of low-noise, low-distortion spectral replication for the detection of a random, nonrepetitive signal. Although we describe the detection of a single pulse, it is not difficult to recognize that spectral cloning can be used for considerably more complex analyses of random events, in both the microwave and optical domains. Besides discriminating noise, the ability to accurately replicate a fast, random event onto an arbitrary frequency map paves the way for low-latency, computation-

free Fourier processing beyond simple coherent summation.

REFERENCES AND NOTES

1. J. R. Lakowicz, *Principles of Fluorescence Spectroscopy* (Springer, New York, 2006).
2. D. Thornton *et al.*, *Science* **341**, 53–56 (2013).
3. G. J. Pendock, D. D. Sampson, *IEEE Photon. Technol. Lett.* **7**, 1504–1506 (1995).
4. R. N. McDonough, A. D. Whalen, *Detection of Signals in Noise* (Academic Press, San Diego, CA, 1995).
5. W. A. Gardner, A. Napolitano, L. Paura, *Signal Process.* **86**, 639–697 (2006).
6. A. Jolly, J. F. Gleyze, J. C. Jolly, *Opt. Commun.* **264**, 89–96 (2006).
7. W. R. Donaldson, J. R. Marcianite, R. G. Roides, *IEEE J. Quantum Electron.* **46**, 191–196 (2010).
8. Z. Tong, S. Radic, *Adv. Opt. Photon.* **5**, 318–384 (2013).
9. J. B. Allen, *IEEE Trans. Acoust. Speech Signal Process.* **25**, 235–238 (1977).
10. Y. Rozanov, *Probability Theory, Random Processes and Mathematical Statistics* (Springer, New York, 1995).
11. R. H. Walden, *IEEE J. Sel. Areas Comm.* **17**, 539–550 (1999).
12. B. Murmann, *ADC Performance Survey 1997–2015*; available at <http://web.stanford.edu/~murmann/adcsurvey.html> (2015).
13. G. W. Anderson, D. C. Webb, A. E. Spezio, J. N. Lee, *Proc. IEEE* **79**, 355–388 (1991).
14. C.-S. Bres, A. O. J. Wiberg, S. Zlatanovic, S. Radic, *J. Lightwave Technol.* **30**, 3192–3198 (2012).
15. M. E. Marhic, *Optical Parametric Amplifiers, Oscillators and Related Devices* (Cambridge Univ. Press, 2008).
16. Z. Tong *et al.*, *Nat. Photonics* **5**, 430–436 (2011).
17. J. D. Taylor, *Ultrawideband Radar: Applications and Design* (CRC Press, 2012).

18. C. Weitkamp, *Lidar: Range-Resolved Optical Remote Sensing of the Atmosphere* (Springer, New York, 2014).
19. E. Myslivets, B. P.-P. Kuo, N. Alic, S. Radic, *Opt. Express* **20**, 3331–3344 (2012).
20. V. Ataie, E. Myslivets, B. P.-P. Kuo, N. Alic, S. Radic, *J. Lightwave Technol.* **32**, 840–846 (2014).
21. Material and methods are available as supplementary materials on Science Online.

22. G. Jacobsen, *Noise in Digital Optical Transmission Systems* (Artech House, Boston, 1994).

ACKNOWLEDGMENTS

This work is funded in part by the Defense Advanced Research Projects Agency. University of California has filed a patent on the method and applications of random signal detection and coherent analysis.

SUPPLEMENTARY MATERIALS

www.sciencemag.org/content/350/6266/1343/suppl/DC1
Materials and Methods
Figs. S1 to S7
References (23–29)

20 August 2015; accepted 12 October 2015
10.1126/science.aac8446

SURFACE SCIENCE

Electron-hole pair excitation determines the mechanism of hydrogen atom adsorption

Oliver Bünermann,^{1,2,3*} Hongyan Jiang,¹ Yvonne Dorenkamp,¹
Alexander Kandratsenka,^{1,2} Svenja M. Janke,^{1,2} Daniel J. Auerbach,^{1,2} Alec M. Wodtke^{1,2,3}

How much translational energy atoms and molecules lose in collisions at surfaces determines whether they adsorb or scatter. The fact that hydrogen (H) atoms stick to metal surfaces poses a basic question. Momentum and energy conservation demands that the light H atom cannot efficiently transfer its energy to the heavier atoms of the solid in a binary collision. How then do H atoms efficiently stick to metal surfaces? We show through experiments that H-atom collisions at an insulating surface (an adsorbed xenon layer on a gold single-crystal surface) are indeed nearly elastic, following the predictions of energy and momentum conservation. In contrast, H-atom collisions with the bare gold surface exhibit a large loss of translational energy that can be reproduced by an atomic-level simulation describing electron-hole pair excitation.

Adsorption of atomic hydrogen (H) is the simplest reaction in surface chemistry. Langmuir's study of this reaction ushered in the era of modern surface science (1). Hydrogen adsorption is important for many fields, ranging from heterogeneous catalysis (2) to interstellar molecular hydrogen production (3). Adsorbed H atoms can stabilize surfaces of intrinsically reactive solids, healing dangling bonds and making them suitable for industrial processing (4). Adsorption is also central to hydrogen storage technologies (5), and it is the basis for a chemical means of manipulating the band gap in graphene (6).

Despite more than a century of study, we still do not have a fundamental understanding of how H-atom adsorption takes place. Adsorption involves the H atom coming to rest at the surface, losing its initial translational energy, and dissipating the energy of the chemical bond formed with the solid (Fig. 1A). Because of its light mass, energy and momentum conservation requires that the transfer of H-atom translational energy to heavy surface atoms is inefficient; for exam-

ple, an H atom colliding with a gold atom at a Au(111) surface is expected to transfer only 2% of its translational energy per collision (Fig. 1B). How then can the H atom lose sufficient translational energy to adsorb? As early as 1979, speculations were made, supported by theoretical analysis, that the mechanism of H-atom adsorption at metals could involve the conversion of H-atom translational energy to electronic excitation of the solid (7). This requires a failure of the

Born-Oppenheimer approximation (BOA), which assumes that electronic motions are much faster than nuclear motions and can be treated separately (8). Although failure of the BOA is not without precedence—for example, infrared linewidths of chemisorbed H atoms on metals are believed to be broadened by electronic interactions (9), and “chemicurrents” have been detected at Schottky diode junctions (10–12)—there are no experimental measurements of the translational inelasticity of H atoms with any solid. Moreover, translational excitation of electron-hole pairs occurring because of collisions of atoms or molecules with surfaces has never been observed in the absence of efficient phonon excitation (13).

Previous experiments on BOA failure showed that highly vibrationally excited molecules exhibit efficient vibrational relaxation when they collide with a clean single-crystal metal surface, whereas little relaxation is seen with insulators (14, 15). This comparison showed the importance of electronic excitation by molecular vibration, a phenomenon that could also be investigated with first-principles theory (16, 17). Although vibrational relaxation studies tell us nothing about adsorption, they suggest an approach to the problem. If BOA failure were important in H-atom adsorption, we would expect inelastic H-atom scattering from metals and insulators to exhibit dramatic differences in their translational energy loss; furthermore, we could only describe the inelasticity with modern theoretical methods that account for electronic excitation (18–20).

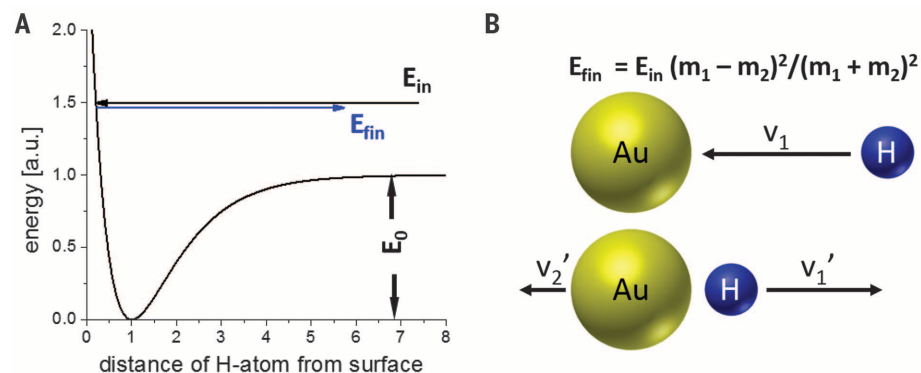


Fig. 1. Adsorption of H atom requires loss of translational energy. (A) The incident H atom must lose its initial translational energy, E_{in} , and dissipate the chemical potential energy, E_0 , that it discovers in binding to the surface. (B) Conserving linear momentum and translational energy in a simple collinear binary collision model leads to a simple relation between E_{in} and the final kinetic energy of the H atom, E_{fin} , that depends only on the masses of the atoms. For the example of H ($m_1 = 1$) colliding with Au ($m_2 = 198$), the H atom retains 98% of its initial energy.

¹Institute for Physical Chemistry, Georg-August University of Göttingen, Tammannstrasse 6, 37077 Göttingen, Germany.

²Department of Dynamics at Surfaces, Max Planck Institute for Biophysical Chemistry, Am Faßberg 11, 37077 Göttingen, Germany. ³International Center for Advanced Studies of Energy Conversion, Georg-August University of Göttingen, Tammannstrasse 6, 37077 Göttingen, Germany.

*Corresponding author. E-mail: oliver.buenermann@chemie.uni-goettingen.de



Subnoise detection of a fast random event

V. Ataie *et al.*

Science **350**, 1343 (2015);

DOI: 10.1126/science.aac8446

This copy is for your personal, non-commercial use only.

If you wish to distribute this article to others, you can order high-quality copies for your colleagues, clients, or customers by [clicking here](#).

Permission to republish or repurpose articles or portions of articles can be obtained by following the guidelines [here](#).

The following resources related to this article are available online at www.sciencemag.org (this information is current as of December 10, 2015):

Updated information and services, including high-resolution figures, can be found in the online version of this article at:

<http://www.sciencemag.org/content/350/6266/1343.full.html>

Supporting Online Material can be found at:

<http://www.sciencemag.org/content/suppl/2015/12/09/350.6266.1343.DC1.html>

A list of selected additional articles on the Science Web sites **related to this article** can be found at:

<http://www.sciencemag.org/content/350/6266/1343.full.html#related>

This article **cites 20 articles**, 1 of which can be accessed free:

<http://www.sciencemag.org/content/350/6266/1343.full.html#ref-list-1>

This article has been **cited by** 1 articles hosted by HighWire Press; see:

<http://www.sciencemag.org/content/350/6266/1343.full.html#related-urls>

This article appears in the following **subject collections**:

Techniques

<http://www.sciencemag.org/cgi/collection/techniques>